Anomalous Microscopic Dielectric Response of Dipolar Solvents and Water

Edward L. Mertz*

National Institute of Child Health and Human Development, National Institutes of Health, Department of Health and Human Services, Bldg. 9, Rm. 1E125, Bethesda, Maryland 20892-0924

Received: July 1, 2004; In Final Form: September 24, 2004

This paper reports measurements of static microscopic dielectric response of several dipolar solvents to charge redistribution in a fluorescent probe. Contrary to recent predictions of dielectric theories and computer simulations of bulk liquids, the observed dielectric response of most solvents conforms to the macroscopic continuum description even at atomic distances, as if these solvents had no spatial intermolecular structure. Such conformance is observed for several probes when the contribution of specific probe−solvent interactions to the response is negligible. However, water, formamide, and glycerol exhibit anomalous responses even though such a probe is used. We discuss a possible reason for the macroscopic-like behavior and a connection between the anomaly and fluctuating structures formed by anomalous solvents near the hydrophobic surface of the probe.

1. Introduction

In biology and chemistry, many reactions and interactions between molecules occur in a solvent. At the most, relevant molecular-scale electrostatic interactions are determined by microscopic dielectric properties of the solvent. A variety of methods, from equilibrium electrochemistry[1,2] and time-resolved nonlinear spectroscopy[3−17] to theory[18−37] and computer simulations combined with quantum chemical calculations,[38−46] provided many insights into inherently complex solvation phenomena. The importance of other nondielectric contributions from specific solute−solvent interactions (hydrogen bonds,[43] dispersive interactions,[18,47] electrostriction and nonlinear response,[48,49] preferential solvation,[50] etc.) was also demonstrated. Molecular liquid theories and simulations were quite successful in describing solvation energetics and can provide a detailed picture of dielectric solvation of many computationally affordable systems. Yet, it has always been desirable to have simpler and faster models.

A simple macroscopic dielectric description of microscopic-scale phenomena is built into widely used models, including quantum chemical programs. It has been applied to static and more complex[51] time-dependent phenomena.[52,53] However, even in the static case, the question of the applicability of macroscopic description at the microscopic scale remains controversial both from experimental and theoretical points of view.

Numerous experimental studies suggested good agreement with macroscopic description, while examples of failure of macroscopic description are also numerous. There may be several reasons for such failure: Most experimental techniques rely on measurement of solvent dielectric response to an electronic structure change in a solute molecule, which is used as a probe. Such molecular probes can be involved in a variety of specific solute−solvent interactions, which may obscure and/or contribute to dielectric response. Furthermore, some physical parameters used to monitor dielectric properties may be more sensitive to specific, nondielectric contributions than others. Even poor approximations within the macroscopic description may cause apparent failure (Section 5).

* E-mail: mertze@mail.nih.gov.

However, if we discard the cases where such obscuring factors are important, we notice that the macroscopic continuum model describes the measured microscopic energies of static dielectric response of most dipolar[54] solvents reasonably well. Such macroscopic continuum-like behavior of solvents, which are molecular and structured in nature, results in the following paradox.

According to rigorous theory[55−57] confirmed by liquid theories,[26,27,36,58] molecular simulations,[59,60] neutron scattering data,[60] and experiments,[11] dielectric properties are intrinsically related to solvent structure. Then, if the characteristic length of solute charge redistribution matches that of the solvent structure, response energies should strongly deviate from macroscopic predictions. The paradox that deviations are expected but not observed was previously explained by the weak sensitivity of experimental probes to solvent structure (due to the probes' large size or large characteristic scale of charge redistribution) or by accidental compensation effects.

In this work, we demonstrate that such an explanation does not resolve the paradox for at least some probes studied previously. Furthermore, we report measurements of static dielectric response energies of dipolar solvents for a dielectric probe proflavine, which should be even more sensitive to solvent structure than traditional dipolar or ionic probes. The largely quadrupolar charge redistribution along the plane of the thin molecule of proflavine (thickness $\approx$ 3.6 Å) occurs on structural length scales of studied solvents. Still, the macroscopic description works for most dipolar solvents. Macroscopic-like behavior of so many different solvents observed for several microscopic probes is difficult to explain by accidental compensation effects, unless there is some physics behind it.

However, our data indicate that such physics may be quite complex. Measurements with our probe indicate that, unlike most hydrogen-bonding solvents, water, formamide, and glycerol exhibit an anomalous dielectric response, which cannot be described in terms of their macroscopic properties even qualitatively. We argue that the anomaly is related to solvent structure and its ability to form 3D networks of hydrogen bonds rather than to specific probe−solvent interactions. But the relationship cannot be explained by the existing nonlocal models (Section 2.2) of structured dielectrics, either. Finally, we suggest a

10.1021/jp047091x
Published on Web 12/13/2004

hypothesis explaining the paradox and discuss the dielectric anomaly.

2. Methods

2.1. Experimental. Visible absorption and corrected fluorescence spectra of proflavine (PF) solutions (concentration < 10 μM) were recorded in 10 × 10 mm^2 quartz cell in absorption (V-560, Jasco Inc.; Lambda 40P, Perkin-Elmer, Inc.) and fluorescence (FP-750, Jasco Inc.; Hitachi 850, Hitachi, Inc.) spectrometers using standard procedures, as described previously.[61] Pressure dependence of the solvent reorganization energy was monitored via emission and fluorescence excitation (directly related to absorption) spectra in an SLM8000 fluorescence spectrometer equipped with a high-pressure cell (Aminco, Inc.). Infrared spectra of PF solutions (concentration < 5 mM) were recorded in a variable path length (<10 μm) CaF_2 cell (Specac, Inc.) with 1 cm^{-1} resolution on a Nexus 670 FTIR spectrometer (Thermo Nicolet, Inc.). Spectra of pure solvents were subtracted in all cases. The optical cells were thermostated to at least ±0.2 °C.

To ensure that PF is in the monocationic form in the ground and excited states,[62] PF solutions were titrated with H_2SO_4 or HBF_4 (up to concentration of ~100 μM) until no traces (to within 2%) of the other protonation forms were detected in the absorption and emission spectra in the 200−800 nm range (spectra of the different forms are shifted by ~50 nm from each other and have orders of magnitude different fluorescence quantum yields). Further 10-fold or higher increase in acid concentration did not affect the spectra. Preparation of PF in a single, monocationic form was possible, because different protonation forms have substantially different pK values (pK_1 = 9.7/12.7, pK_2 = 0.2/1.5, and pK_3 ≈ −0.5 for the ground/excited state of PF in water[63]). Ion pairs between PF and solution counterions were not detected in the spectra either. PF concentrations were low enough to avoid aggregation.

Spectra of deuterated PF were recorded in D_2O, $HCOND_2$ (formamide), CH_3OD, C_2H_5OD, and $SO(CH_3)_2$ (anhydrous dimethyl sulfoxide) titrated with concentrated D_2SO_4, resulting in >97% of titratable D atoms. These solutions were prepared from PF hydrochloride deuterated by dissolving in CH_3OD and subsequent drying under vacuum.

Solvents of the highest commercially available purity were used. Proflavine hydrochloride (CAS no. 952-23-8), acridine orange hydrochloride hydrate, and coumarin-153 were purchased from Aldrich.

2.2. Theory. *Spectroscopic Method.* Our spectroscopic evaluation of microscopic dielectric response energies of solvents is based on the measurement of solvent dependence of the absorption and steady-state emission spectra of a fluorescent probe.[64] Briefly, absorption of a photon leads to rapid (~1 fs) electron density redistribution $\Delta\rho_a$ in the probe, Figure 1a. This transition between the ground state and the lowest singlet excited state is followed by much slower relaxation of the chemical bonds in the dye and relaxation/reorganization of the solvent (less than 10 ps). During such a reorganization, the dye can emit photons as a result of the reverse transition between the same excited and ground states. Because the lifetime of the excited state (3 ns) is 3 orders of magnitude longer than the relaxation times, most photons (~99.9%) are emitted after the relaxation is complete. After the emission, the reverse charge redistribution $\Delta\rho_e \approx -\Delta\rho_a$ causes similar reorganization of the solute and solvent, and the system returns to the equilibrium ground sate. As a result, the solvent dielectric response associated with the solvent reorganization has a substantial effect

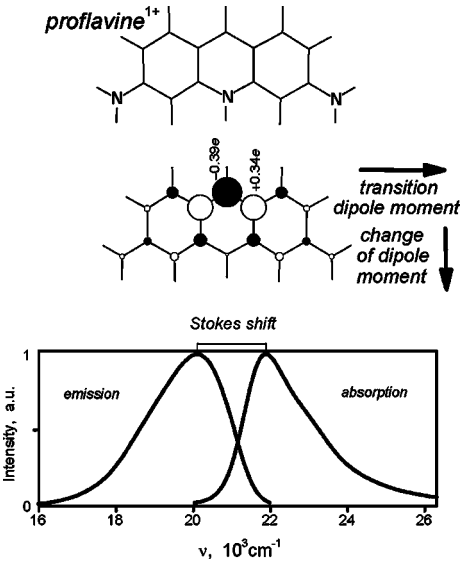

Figure 1. (Top) Quadrupolar-like electron density redistribution of a dielectric probe, monocationic proflavine, caused by light absorption. This redistribution rapidly varies along the molecular plane and has a low dipolar component (1.2 Debye). It is obtained from CIS/6-31G(d,p) quantum chemical calculations and then approximated by changes in atomic charges. Filled and hollow circles illustrate negative and positive changes in charges. The radius of each circle is proportional to the change. (Bottom) Absorption and steady-state emission spectra of proflavine in methanol. As described in the text, the Stokes shift is related to the energy λ_s of the solvent dielectric response to proflavine charge redistribution.

on the absorption and emission spectra of the dye. In particular, the maxima of the absorption ν_a and emission ν_e spectra are related to solvent response via the equilibrium free energy gap ΔG between the ground and excited states and the solvent reorganization energy λ_s.[65]

$$h\nu_a \approx \Delta G + \lambda_{ia} + \lambda_s - M_{3a}/2M_{2a}$$

$$h\nu_e \approx \Delta G - \lambda_{ie} - \lambda_s + M_{3e}/2M_{2e}$$

$$h\nu_a - h\nu_e \approx 2(\lambda_i + \lambda_s) - M_{3a}/2M_{2a} + M_{3e}/2M_{2e} \quad (1)$$

Here, $h\nu_a - h\nu_e$ is the Stokes shift, h is the Planck's constant, $\lambda_i = (\lambda_{ia} + \lambda_{ie})/2$ is the intramolecular reorganization energy of the dye, and M_2 and M_3 are the second and third moments of the absorption (a) and emission (e) spectra, correspondingly.

Interpretation of $\Delta G \approx (h\nu_a + h\nu_e)/2$ related to the difference in solvation energies of the ground and excited states may be nontrivial, because ΔG may have nondielectric contributions. For example, significant contributions may be caused by changes in the dispersion dye−solvent interactions[18,66,67] due to different electronic polarizabilities of the ground and excited states or by the interaction between charge redistribution and solvent potential pre-existing before the transition.[39,68−72] The latter potential may by be caused not only by solvent polarization produced by solute charges but also by solute−solvent hydrogen bonding, solvent packing constraints near solute cavity, and so on.

In this work, we focus on the solvent reorganization energy λ_s, a characteristic of solvent dielectric response which is less sensitive to such nondielectric contributions[18,67,68] (Section 3 and Supporting Information). In practice, some assumptions and approximations are required to extract λ_s from the spectra. To minimize potential errors introduced by such procedures (e.g., by extrapolation of the wings of the spectra), we used three different parameters to monitor λ_s (i.e., the Stokes shifts of the

first moments of absorption and emission spectra, M_{2a} and M_{2e}; M_2 is related to the half-width of spectral band and, thus, also to λ_s).[65] For qualitative evaluation, we used the Stokes shift of the maxima $h\nu_a - h\nu_e \approx 2(\lambda_i + \lambda_s)$[28,64,65] and assumed that λ_i is similar in different solvents (this assumption is verified in Section 3.3 and Sections 1.5S and 3.4S in the Supporting Information). For more quantitative estimates, we accounted for the contribution of the spectral moments by following a few different procedures to extract M_2 and M_3 (e.g., by direct integration of the spectra or by fitting the band shape functions[61,65]). All approaches produced consistent results.

Energy of Linear Dielectric Response. If contributions from specific solute−solvent interactions are negligible, the solvent reorganization energy λ_s is related to the total energy W of the linear, static solvent dielectric response[24,25,64]

$$\lambda_s = W - W_{op}, \quad W = -\frac{1}{2}\int d\mathbf{r}\Delta\varphi(\mathbf{r})\Delta\rho(\mathbf{r})$$

W is related to the change $\Delta\varphi$ in equilibrium electric potential of solvent induced by solute charge redistribution $\Delta\rho$. Unlike W, the solvent reorganization energy λ_s has no contribution from solvent electronic polarization W_{op} (W_{op} is similarly related to the potential $\Delta\varphi_{op}$ of electronic polarization induced by $\Delta\rho$, $W_{op} = -\int d\mathbf{r}\Delta\varphi_{op}\Delta\rho/2$).[24,25] This is because the solvent electronic polarization is always in equilibrium with the solute charge redistribution due to relaxation time of the electronic polarization (∼0.1 fs) being much shorter than the time of photon absorption/emission (∼1 fs). As a consequence of such separation of time scales, λ_s is independent of relaxational or other time-dependent parameters of the solvent.[25,64] Note also that λ_s values for absorption and emission are similar, because charge redistributions are similar ($\Delta\rho_a \approx -\Delta\rho_e$, verified in Section 3 and Supporting Information) and W does not depend on the sign of $\Delta\rho$.

Microscopic Dielectric Response and Solvent Structure. The response energy W can be also expressed in terms of the change in solvent polarization $\Delta\mathbf{P}$ induced by the change in solute electric field $\Delta\mathcal{E}$ produced by the solute charge redistribution $\Delta\rho$ in a vacuum ($\mathrm{div}\Delta\mathcal{E} = 4\pi\Delta\rho$)[68−71,73,74]

$$W \equiv \frac{1}{2}\int d\mathbf{r}\Delta\mathbf{P}\Delta\mathcal{E}$$

The fluctuation dissipation theorem relates the induced polarization $\Delta\mathbf{P}$ to solvent polarization fluctuations $\delta\mathbf{P}$ and $\Delta\mathcal{E}$ via the static susceptibility tensor, $\gamma_{\alpha\beta}(\mathbf{r}, \mathbf{r}') = 4\pi/T\langle\delta P_\alpha(\mathbf{r})\,\delta P_\beta(\mathbf{r}')\rangle$[55−57,75,76]

$$4\pi\Delta P_\alpha(\mathbf{r}) = \sum_\beta\int\gamma_{\alpha\beta}(\mathbf{r}, \mathbf{r}')\Delta\mathcal{E}_\beta(\mathbf{r}')\,d\mathbf{r}' = \sum_\beta\int\chi_{\alpha\beta}(\mathbf{r}, \mathbf{r}')\Delta\mathbf{D}_\beta(\mathbf{r}')\,d\mathbf{r}'$$

where $\langle\ \rangle$ denotes ensemble average in the absence of applied field $\Delta\mathcal{E}$; $\alpha, \beta = x, y, z$; T is temperature in energy units; $\Delta\mathbf{D}$ is the change in electric induction, $\Delta\mathbf{D} \equiv \Delta\mathbf{E} + 4\pi\Delta\mathbf{P} \equiv \Delta\mathcal{E} + \mathbf{E}(\Delta\mathbf{P}) + 4\pi\Delta\mathbf{P}$ with $\mathbf{E}(\Delta\mathbf{P})$ being the electric field produced by induced polarization $\Delta\mathbf{P}$; and $\chi_{\alpha\beta}(\mathbf{r}, \mathbf{r}')$ is the response tensor.

In the static response of liquids, solvent molecules have enough time to sample space on the length scale of solvent structure, resulting in a continuum-like response of molecular solvent.[33−35,37] Nevertheless, the spatial correlator of polarization fluctuations retains information about pair correlations between orientations of solvent dipoles and, thus, about short-range, microscopic solvent structure and long-range correlations due to electrostatic dipole−dipole interactions.[55,56,76−80] As a result, susceptibility tensor $\gamma_{\alpha\beta}(\mathbf{r}, \mathbf{r}')$ depends on the overall geometry of the dielectric material, and electrostatics operates with a more invariant characteristic, response tensor $\chi_{\alpha\beta}(\mathbf{r}, \mathbf{r}')$, which relates $\Delta\mathbf{P}$ and the change in electric induction $\Delta\mathbf{D}$. Because the ensemble average $\langle\delta P_\alpha(\mathbf{r})\,\delta P_\beta(\mathbf{r}')\rangle$ over all solvent configurations does not invoke coarse-graining over macroscopic volumes, these dielectric relationships are microscopic and account for both translational and rotational degrees of freedom of solvent molecules.

The response tensor $\chi_{\alpha\beta}(\mathbf{r}, \mathbf{r}')$ is intrinsically related to polarization fluctuations and $\gamma_{\alpha\beta}(\mathbf{r}, \mathbf{r}')$, but the general form of this relationship is not known.[76] Several models of $\chi_{\alpha\beta}(\mathbf{r}, \mathbf{r}')$ were used in the literature, but none of the existing models has been rigorously justified for dipolar dielectrics at the microscopic scale (except for a uniform isotropic dielectric).

Macroscopic Dielectric Continuum Model (DCM). The DCM assumes that the solvent has no spatial structure on the length scale of the spatial variation of $\Delta\mathcal{E}(\mathbf{r})$, so that $\chi_{\alpha\beta}(\mathbf{r}, \mathbf{r}')$ can be approximated by $\chi_{\alpha\beta}(\mathbf{r}, \mathbf{r}') \neq \chi\delta_{\alpha\beta}\,\delta(\mathbf{r} - \mathbf{r}')$ ($\delta_{\alpha\beta}$ and $\delta(\mathbf{r} - \mathbf{r}')$ are the Kronecker's symbol and Dirac's delta functions).[55,56,76,81] This approximation of classical electrostatics reduces the relationship between $\Delta\mathbf{P}$ and $\Delta\mathbf{D}$ to the local, macroscopic form, $4\pi\Delta\mathbf{P} = \chi\Delta\mathbf{D}$. Thus, macroscopic electrostatics is expected to work well when the short-range part of the correlator $\langle\delta P_\alpha(\mathbf{r})\,\delta P_\beta(\mathbf{r}')\rangle$ in the solvent has a much shorter length scale than the characteristic length scale of the electric field variation.

One may expect that the short-range part of polarization fluctuations $\langle\delta P_\alpha(\mathbf{r})\,\delta P_\beta(\mathbf{r}')\rangle$ extends to at least the size of the solvent molecule. In dipolar solvents, the correlation range may be even larger because of strong intermolecular interactions resulting in intermolecular structuring of solvent molecules. Early treatments assumed a simple exponential form for the short-range part which is proportional to $e^{-|\mathbf{r}-\mathbf{r}'|/l}$ (Lorentzian approximation[55,56,82−84]). The presence of more complex structures in various dipolar solvents was demonstrated later by several approaches based on phenomenological[85] and molecular[26,27,36,58] theories, simulations,[59,60] and neutron scattering data.[60] Then, the simple DCM approximation should not work.

The response tensor of molecular solvents is essentially nonlocal $\chi_{\alpha,\beta}(\mathbf{r}, \mathbf{r}') \neq \chi\delta_{\alpha\beta}\,\delta(\mathbf{r} - \mathbf{r}')$. For example, for a uniform isotropic dielectric material, longitudinal parts of $\chi_{\alpha\beta}$ and $\gamma_{\alpha\beta}$ are related to the nonlocal isotropic response function $\chi(\mathbf{r} - \mathbf{r}')$, $\chi^L{}_{\alpha\beta}(\mathbf{r}, \mathbf{r}') = \gamma^L{}_{\alpha\beta}(\mathbf{r}, \mathbf{r}') \propto \chi(\mathbf{r} - \mathbf{r}')$.[55,56,86] In this case, W and solvent reorganization energy λ_s can be expressed in terms of Fourier transforms $\Delta\mathcal{E}(\mathbf{k})$ of $\Delta\mathcal{E}(\mathbf{r})$ and the nonlocal isotropic response function $\chi(\mathbf{r} - \mathbf{r}')$[25,27,38,76,83,84,87]

$$\lambda_s = \frac{1}{64\pi^4}\int d\mathbf{k}[\chi(k) - \chi_{op}]\Delta\mathcal{E}(\mathbf{k})^2, \qquad W = \frac{1}{64\pi^4}\int d\mathbf{k}\chi(k)\Delta\mathcal{E}(\mathbf{k})^2 \quad (2)$$

where $\chi(k) = 1 - 1/\epsilon_{st}(k)$, $\chi_{op} = 1 - 1/\epsilon_{op}$, and $\epsilon_{st}(k)$ and ϵ_{op} are the static and optical (high-frequency) dielectric constants. In Fourier space, nonlocal response is associated with k-dependence of $\chi(k)$, $\chi(k) \neq$ const., Figure 6a. When a kth component of the electric field produced by solute charge redistribution $\Delta\rho$ matches the quasiperiodicity ($2\pi/k$) of a structured solvent, a resonant dielectric response can occur. At the resonance, $\chi(k)$, and, thus, dielectric response energy, can exceed the macroscopic limit of $\chi = 1$ by several orders of magnitude.

Nonlocal Dielectric Models. The response tensor near a solute may be different from the bulk response tensor $\chi_{\alpha\beta}(\mathbf{r} - \mathbf{r}')$, $\chi_{\alpha\beta}(\mathbf{r}, \mathbf{r}') \neq \chi_{\alpha\beta}(\mathbf{r} - \mathbf{r}')$, because the presence of the solute cavity breaks the isotropic symmetry of the solvent. Several models relating $\chi_{\alpha\beta}(\mathbf{r}, \mathbf{r}')$ to the bulk function $\chi(\mathbf{r} - \mathbf{r}')$ were proposed or borrowed from plasma physics.[55,56,76] The "smeared charge" model assumes that solvent freely permeates inside the solute and that bulk solvent properties are not perturbed, $\chi_{\alpha\beta}(\mathbf{r}, \mathbf{r}') = \chi_{\alpha\beta}(\mathbf{r} - \mathbf{r}')$ (eq 2).[55,56,83,84] Finite cavity size is accounted for by smearing solute charges around a volume of which the size is comparable to the solute size. "Dielectric approximation" assumes that the dielectric tensor $\epsilon_{\alpha\beta}(\mathbf{r}, \mathbf{r}')$ is not perturbed by the solvent-impermeable cavity ($\epsilon_{\alpha\beta}(\mathbf{r}, \mathbf{r}') = \epsilon_{\alpha\beta}(\mathbf{r} - \mathbf{r}')$).[88] The "specular reflection" model derives the strongly perturbed dielectric function $\epsilon_{\alpha\beta}(\mathbf{r}, \mathbf{r}') \neq \epsilon_{\alpha\beta}(\mathbf{r} - \mathbf{r}')$ by assuming that solvent polarization is zero at the boundary of the solvent-impermeable cavity.[89] However, application of such models to dipolar liquids is purely heuristic, because none of them has been derived for dipolar dielectrics.[55,56,76]

2.3. Calculations. *Quantum Chemical Calculations.* Ab initio quantum chemical calculations were performed for spectroscopic probes proflavine monocation (PF) and coumarin-153 (C153) in the ground state and the first excited state and for electrochemical probe cobaltocene (Cp_2Co) in three redox ground states. We used the calculations to analyze experimental solvent dielectric response energies within dielectric models and to characterize PF. *Gaussian* program (versions 98 and 03, revisions A.11 and B.03, respectively) was used.[90]

Most calculations of the reorganization energies were done within density functional theory (DFT) with the time-dependent (TD) approach[91] to the excited states. Because TDDFT analysis of excited-state electron densities is not accessible within existing *Gaussian* versions, the single-excitation configuration interaction (CIS) approach was also used and compared with TDDFT, whenever possible.

Calculations of PF were done with the 6-31G(d,p) basis set and MPW1PW91 functional, which showed good performance for excited states of various molecules.[92−94] Such calculations produced good agreement with experimental data on the vertical transition energy, transition dipole moment, and intramolecular and solvent reorganization energies (see Supporting Information Tables 1S and 2S). Usage of larger basis sets had a small effect on the reorganization energy (and on other characteristics), because this energy is related to the energy difference for the same electronic state (Table 2S). CIS, time-dependent Hartree−Fock (TDHF), and TDDFT schemes produced similar characteristics including the change of dipole moment upon the transition.

Calculations of PF in supermolecular complexes with solvent molecules were performed in order to model various effects of specific solute−solvent interactions (hydrogen bonding and electron donor−acceptor interactions). This modeling included 6-31G(d,p)/B3LYP[95,96] calculations of the vibrational spectra of PF and the assignment of vibrations on the basis of experimental infrared spectra of normal and deuterated PF (this work) and with resonance Raman spectra of PF[97,98] (Section 2S, Supporting Information).

Calculations of the syn conformation of C153 were mainly done within the MPW1PW91/6-31G(d,p) scheme which demonstrated good performance for excited states of coumarins.[94] The CIS/6-31G(d,p) scheme produced similar solvent reorganization energies (uniformly 1.5 times higher for all solvents) and was used for calculating the electron density redistribution.

Calculations of Cp_2Co in the eclipsed conformation were done within the B3LYP/6-31+G(d,p) scheme. Geometry optimization without symmetry constraints of the charge $z = 0$, total spin $S = {}^1/_2$ state produced interatomic distances within 0.03 Å of those obtained from the gas-phase electron diffraction data[99] (such agreement is considered to be a criterion of applicability of a calculation scheme to metallocences[100]). States ($z = +1$, $S = 0$), ($z = 0$, $S = {}^1/_2$), and ($z = -1$, $S = 1$) were found to be the equilibrium ground states and were used in the dielectric calculations.

Dielectric Continuum Model. Ab initio quantum chemical calculations of the solvent dielectric response energies W and λ_s within DCM were performed without adjustable parameters. The solutes were placed inside the cavities formed in the dielectric continuum whose macroscopic optical ϵ_{op} and static ϵ_{st} dielectric constants of the surrounding dielectric continuum were set to be equal to the experimental values for each solvent. The solute cavity was built using the united atom model approximating heavy atoms with spheres of radii of ~ 2 Å $\times \alpha$ scaled with coefficient $\alpha = 1.4$ (the other limit $\alpha = 1.2$ of the recommended range[101] $\alpha = 1.2-1.4$ was also tested). The effect of solvent reaction field on the solute wave functions was accounted using the integral equation formalism polarized continuum model (IEFPCM) scheme.[102,103]

Within the IEFPCM solvation scheme, the solvent reorganization energy λ_s of the optical transition between the ground state and the first singlet excited state of PF and C153 is evaluated as the difference of two energies:[24,25,102−104] (i) the energy of the excited state with the excited-state equilibrium configuration of the self-consistent reaction field of solvent polarization, (ii) the energy of the excited state with the nonequilibrium configuration of the slow (inertial) polarization fixed at the ground-state equilibrium configuration. Both energies were calculated at the same fixed geometry (mainly the ground-state gas-phase geometry; other geometries produced similar results).

The total energy of dielectric response W for Cp_2Co was determined as the energy differences $W = {}^1/_2[\Delta U(z = +1, S = 0) + \Delta U(z = -1, S = 1)]$ (where $\Delta U(z, S) = U^{gas} - U^{solv}$, U^{gas}, and U^{solv} are energies of different redox states of Cp_2Co in the gas phase and in solvent). DFT/B3LYP/6-31+G(d,p) calculations of all redox states were performed at the same fixed geometry optimized for the ground ($z = 0$, $S = {}^1/_2$) state in the gas phase (usage of ($z = +1$, $S = 0$) or ($z = -1$, $S = 1$) geometry produced similar results).

Nonlocal "Smeared Charge" Model. In lieu of quantum chemical programs implementing nonlocal dielectric models, we analyzed the data within the simplest model of smeared charges in uniform solvent.[55,56,83,84] Solvent-dependent W and λ_s were calculated from eq 2 for the same probes as within DCM. The electric field in eq 2, $\Delta\mathcal{E}(\mathbf{k}) = 4\pi\Delta\rho(\mathbf{k})/i\mathbf{k}$, was conveniently expressed in terms of charge redistribution $\Delta\rho(\mathbf{k})$[76,83,84,87]

$$\lambda_s = \frac{1}{\pi}\int_0^\infty [\chi(k) - \chi_{op}]\Delta\rho(k)^2\, dk, \quad W = \frac{1}{\pi}\int_0^\infty \chi(k)\Delta\rho(k)^2\, dk \tag{3}$$

where $\Delta\rho(k)^2 \equiv \int_0^{2\pi} d\varphi \int_0^\pi \sin\theta\, d\theta\, |\Delta\rho(\mathbf{k})|^2/4\pi$ is $\Delta\rho(\mathbf{k})$, averaged over angles of the spherical coordinate system.

The primary analysis reported in Table 1 and Figures 5 and 6b used no adjustable parameters. The available response functions $\chi(k)$'s of bulk dipolar solvents were taken from ref 58 and used without modification (a few such $\chi(k)$'s are shown in Figure 6a). The electron density redistributions were calculated at fixed gas-phase ground-state geometries of PF and C153

[$\Delta\rho = (\rho(S_1) - \rho(S_0)$] and ($z = 0$, $S = {}^1/_2$)-state geometry of Cp_2Co [$\Delta\rho(\mathbf{r}) = \rho(z = 0, S = {}^1/_2) - \rho(z = +1, S = 0)$]. We used solvent-independent $\Delta\rho = \Delta\rho(\epsilon_{op} = 2.05/\epsilon_{st} = 37)$ obtained within the nonequilibrium IEFPCM/CIS/6-31G(d,p) for PF and C153 and within the equilibrium IEFPCM/B3LYP/6-31+(d,p) for Cp_2Co solvation schemes (Figure 6b,c). We also verified that the choice of $\Delta\rho$ does not affect the semiquantitative results obtained for the smeared charge model ($\Delta\rho$ obtained from gas-phase calculations $\Delta\rho(\epsilon_{op} = 1, \epsilon_{st} = 1)$, the equilibrium solvation scheme, solvent-dependent $\Delta\rho(\epsilon_{op}, \epsilon_{st})$, or $\Delta\rho(Cp_2Co) = \rho(z = -1, S = 1) - \rho(z = 0, S = {}^1/_2)$ were tested).

Previous applications of the model used adjustable parameters to account for uncertainties in the model parameters.[55,76,83−85,87] In an attempt to improve predictions of the model, we used similar adjustments and modified the primary analysis in three ways: (a) Spatial extent of electron shells is somewhat dependent on the particular method of quantum chemical calculations. Therefore, we varied the effective size and $\Delta\rho(\mathbf{r})$ of the probes by using the Gaussian smearing function $f(\mathbf{r})$ with the same-for-all-solvents adjustable size a

$$\Delta\rho(\mathbf{r}, a) = \int d\mathbf{r}'\Delta\rho(\mathbf{r}')f(\mathbf{r} - \mathbf{r}')$$

$$f(\mathbf{r}) = (2\pi)^{-3/2}a^{-3}\exp(-r^2/2a^2)\ (0 < a < \infty) \qquad (4)$$

Note that $\Delta\rho(\mathbf{r}, a \to 0) = \Delta\rho(\mathbf{r})$.

(b) Response functions somewhat depend on particular approximations of charges of the solvent molecules used for their derivations. To test the sensitivity of the results to peak heights of $\chi(k)$ (i.e., to $\chi(k)$ in the medium and large k-range), the nonlocal part of the response functions $\chi(k) - \chi(0)$ was reduced by the same-for-all-solvents factor b, $\chi(k, b) = \chi(0) - [\chi(k) - \chi(0)]/b$, $(1 < b < \infty)$.

(c) We also tested the Lorentzian approximation introduced in earlier treatments as a small k approximation,[55,82−84] $\chi(k) = 1 - \epsilon_{op}^{-1} + (\epsilon_{op}^{-1} - \epsilon_{st}^{-1})/(1 + l^2k^2)$. In this case, the same-for-all-solvents correlation length l was used as the adjustable parameter.

Finally, for consistent comparison of the nonlocal and DCM models, we also performed DCM calculations within the approximations of the smeared charge model, that is, we set $\chi(k)$ to its macroscopic value $\chi(k) = \chi(0)$.

3. Probe Characterization

Our auxiliary studies indicated that solvent dependence of PF reorganization energy in all studied solvents (including anomalous ones) is determined primarily by solvent dielectric properties rather than by probe- or solvent-specific effects. Briefly, these spectroscopic (visible and infrared) experiments and quantum chemical calculations (QCC) detailed in the Supporting Information showed the following.

Reorganization of PF Geometry. (1) Contribution to the reorganization energy from a shift of dissociation equilibrium upon the optical transition was negligible, because PF was in the same protonation form and did not form ion pairs in the ground and excited states (Section 2.1). (2) The structure and size of the dye change little upon transition, indicating a negligible contribution from energies associated with the formation of the dye cavity as indicated by QCC (Supporting Information Section 3.2S). (3) Intramolecular reorganization energy λ_i varies little from solvent to solvent (by less than 3% of $\lambda_i \approx 900\ cm^{-1}$) (Sections 1.5S and 3.4S in Supporting Information); and coupling between the intramolecular and solvent reorganization is small ($\sim$60 cm^{-1}), as indicated by QCC of solvated PF (Section 1.6S in Supporting Information).

Reorganization of Solvent and Specific Solvent Effects. (4) Most photons ($\sim$99.9%) are emitted by the dye after dielectric relaxation of most solvents is complete, thus energy of static dielectric response is measured as confirmed by auxiliary experiments (Supporting Information Section 3.3S). (5) The main 90% contribution to the dielectric response comes from free rather than bound solvent (most solvent molecules in the first solvation shell do not form hydrogen bonds with the dye) as estimated by QCC (Table 1S and Section 1.7S in Supporting Information). (6) Reorganization of the dye−solvent hydrogen bonds that do form is small: Calculated λ_i values are similar for isolated and solvated PF and for PF in the supermolecular complex with several solvent molecules (probably because the change in electron density at the bonding H atoms is small, see Figures 1 and 6c) (Table 1S in Supporting Information); the absence of the H/D isotope effect on the fine vibronic structure of absorption and emission spectra associated with R−H(D) vibrations indicates a negligible contribution from the dye−solvent hydrogen bonds (Section 3.5S in Supporting Information). (7) Only small effects of PF−solvent interactions on the PF electronic structure and on its change upon excitation were found in QCC of the ground and excited states of PF in the supermolecular complex with several solvent molecules (Table 2S, Sections 3.4S and 3.6S in Supporting Information). (8) We found no indication of specific solvent effects on the PF electronic structure that would be present in nonanomalous solvents and absent in anomalous ones: (a) PF infrared spectra were similar in different solvents (Section 2S), (b) transition dipole moments and the fluorescence quantum yield varied little with solvent and did not correlate with the Stokes shifts and λ values (Section 3.6S), (c) the equilibrium energy gap ΔG between the ground and excited states did not correlate with the Stokes shift (ΔG approximately decreased with the optical dielectric constant ϵ_{op} of the solvent, indicating the expected significant contribution from dye−solvent dispersion interactions, see Figure 5S in Supporting Information).

4. Results

4.1. Experimental. Figure 2 shows that the Stokes shift of PF measured in non-hydrogen-bonding solvents correlates with the solvent reorganization energy λ_s^{cal} calculated within DCM coupled with quantum chemical calculations. A single, dashed curve fits the data points for all solvents. This curve is a prediction of eq 1 with quantum-chemically calculated solvent λ_s, intramolecular λ_i reorganization energies, and measured spectral moments M_2 and M_3. Such an initial prediction produced a reasonable description of the data and, then, was refined by a slight adjustment of λ_s, λ_i, M_2, and M_3 within their experimental errors and uncertainties of calculations by fitting with eq 1 as described previously.[61] In particular, a scaling factor correcting the calculated λ_s^{cal} was introduced, $\lambda_s \approx 1.25\lambda_s^{cal}$. The corresponding data on reorganization energies are summarized and complied in Table 1 and Supporting Information Table 3S and Figure 6S.

The Stokes shifts in linear H-bonding solvents (such as alcohols) also correlate with calculated λ_s values (dotted line), but with the scaling factor and reorganization energy $\lambda = \lambda_i + \lambda_s$ slightly lower than for non-H-bonding solvents (probably because the cationic PF accepts a weak H-bond from a solvent molecule[105]).

However, the Stokes shifts observed in branched H-bonding solvents exhibit deviations from the correlations established

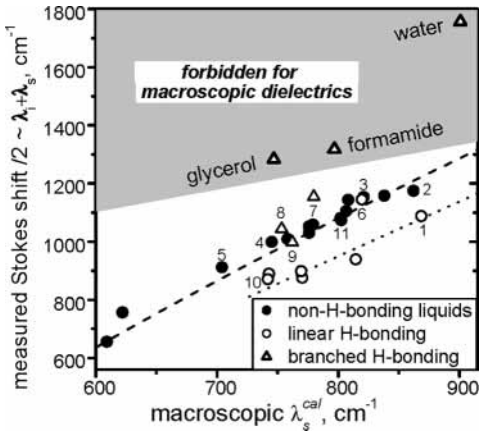

Figure 2. The Stokes shift of proflavine in different solvents at 20 °C vs the macroscopic solvent reorganization energy λ_s^{cal}, calculated from the dielectric constants of each solvent within the TDDFT−quantum chemical approach. (1) methanol, (2) acetonitrile, (3) nitromethane, (4) DMSO, (5) tetramethylene sulfoxide, (6) *N*-methyl formamide, (7) ethylene glycol, (8) 1,2-propanediol, (9) 1,3-propanediol, (10) 2-butanol, and (11) acetone. For glycerol, the Stokes shift extrapolated to infinite lifetime of the excited state is plotted (Supporting Information, Section 3.3S). Other data points show previously studied solvents.[61] The dashed and dotted lines show predictions for non- and linear H-bonding liquids, correspondingly, based on the dielectric continuum model/TDDFT calculations of λ_s^{cal} and the intramolecular reorganization energy λ_i^{cal}. The region forbidden within the dielectric continuum model is estimated on the basis of the macroscopic limits for $\epsilon_{st} = \infty$ and $\epsilon_{op} \geq 1.8$ (water has one of the lowest $\epsilon_{op} \approx 1.8$ for liquids at ambient conditions). The measured λ_s's for water, formamide, and glycerol (obtained from eq 1 and measured spectral moments) are ~1.6, 1.2, and 1.3 times higher than the values expected from their macroscopic dielectric constants.

TABLE 1: Performance of Dielectric Models against Measured Energies of Solvent Dielectric Response[a]

model	local $\chi = \chi(0)$ macroscopic DCM				nonlocal $\chi = \chi(k)$ from molecular simulations	
	solute in cavity		smeared charge[b]		smeared charge	
	$\Delta x/\bar{x}$	$\bar{x}$[e]	$\Delta x/\bar{x}$	$\bar{x}$	$\Delta x/\bar{x}$	$\bar{x}$
proflavine[c]	0.05	0.80−1.07	0.11	1.0	1.33	7
coumarin 153[c]	0.22	0.56−0.76	0.23	1.3	0.89	7
cobaltocene[d]	0.01	0.85−0.97	0.01	1.2	0.14	1.7

[a] For a good model, $\Delta x/\bar{x} \ll 1$ and $\bar{x} \approx 1$. Here, $\Delta x = x_{max} - x_{min}$ and $\bar{x}$ are maximal variation and average values of ratio $x = U^{cal}/U$ of calculated U^{cal} and measured U energies of dielectric response for solutes in a set of nonanomalous solvents ($U = \lambda_s$ for proflavine and coumarin-153; $U = W$ for cobaltocene). [b] DCM calculations without cavity were performed using the nonlocal smeared-charge model but with the DCM response function $\chi(k) = \chi(0) \equiv \chi$; Section 2.3. [c] Set of solvents: acetonitrile, DMSO, acetone, methanol.[132] [d] Set of solvents: acetonitrile, DMSO, acetone.[132] [e] The lower and upper bounds correspond to $\alpha = 1.4$ and 1.2, respectively; Section 2.3.

within DCM for other studied solvents (Figure 2). Such deviations are anomalously high in water, formamide, glycerol, and ethylene glycol. Even if both non- and linear-H-bonding solvents are included in the correlation, deviations of water, formamide, and glycerol exceed 4σ; the deviation of ethylene glycol is $\sim 2.3\sigma$ (σ is standard deviation). Note that we obtained similar correlations and deviations by using the absorption or emission bandwidths to monitor reorganization energy in the studied solvents (the second moments M_2's of the spectra increased monotonically with increasing Stokes shift).

In the anomalous solvents, the reorganization energy has not only abnormally high absolute values but also qualitatively

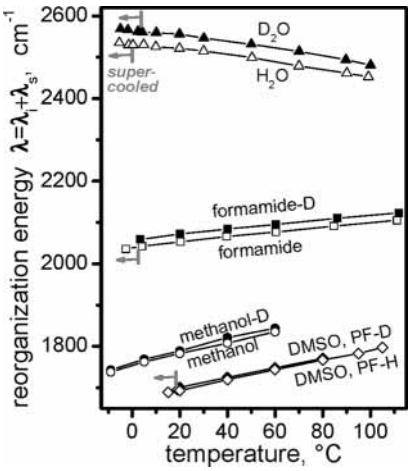

Figure 3. Effects of temperature and solvent isotopic H/D substitution on the measured reorganization energy λ of proflavine. Points along the left-pointing arrows refer to supercooled solvents. λ was obtained from eq 1 using the measured spectral moments M_2 and M_3 and Stokes shift. The isotopic substitution of hydrogens that form H-bonds leads to ~2, 1, and 0% higher λ_s than in nonsubstituted water, formamide, and methanol, respectively.

TABLE 2: Slopes of Measured and Calculated Dependencies of Reorganization Energies on Temperature and Pressure for Proflavine

solvent	$d\lambda/dT$ cm^{-1}/K[a]	$d\lambda_s^{cal}/dT$ cm^{-1}/K[b]	$d\lambda/dP$ $cm^{-1}/kbar$[c]	$d\lambda_s^{cal}/dP$ $cm^{-1}/kbar$[b]
water	-0.84 ± 0.03	0.05	1 ± 5	13
acetonitrile	0.8 ± 0.2	0.14	3 ± 5	23
methanol	1.32 ± 0.02	0.11	9 ± 5	27
DMSO	1.20 ± 0.02	0.36		
formamide	0.59 ± 0.02			

[a] The reorganization energies λ's and their experimental statistical errors measured at $P = 1$ bar. Systematic uncertainty in $d\lambda/dT$ associated with temperature-dependent spectral band shapes is ~0.6 cm^{-1}/K. It is estimated on the basis of different values obtained by different procedures of evaluating λ; Section 2.2. [b] The solvent reorganization energy λ_s^{cal} is calculated within TDDFT/MPW1PW91/6-31G(d,p)/IEFPCM scheme with $\alpha = 1.4$ (Section 2.3). [c] The reorganization energies λ's and their experimental statistical errors measured at 20 °C.

different dependencies on temperature, solvent isotopic substitution, and cosolvent concentration.[106] Specifically, the measured reorganization energy $\lambda = \lambda_i + \lambda_s$ in nonanomalous solvents increases with temperature, as shown, for example, for methanol and dimethyl sulfoxide (DMSO) in Figure 3 and Table 2. However, it decreases with temperature in water and weakly depends on temperature in formamide.

H → D isotopic substitution of solvent and PF hydrogen atoms capable of forming hydrogen bonds (H_nO and H_nN atoms; $n = 1, 2$) has a very small effect on λ measured in nonanomalous non- and linear H-bonding solvents (e.g., for DMSO and methanol, λ increases by ~5 cm^{-1}, see Figure 3). This is expected on the basis of a very small isotope effect on the macroscopic dielectric constants of solvents. However, λ increases by ~18 cm^{-1} upon H → D substitution in formamide. The solvent isotope effect becomes even more anomalous in water (~35 cm^{-1}).

The isotope effect in λ may be caused by changes in dielectric reorganization of the solvent, PF molecule, or PF−solvent hydrogen bonds. However, we believe that the observed effect in water and formamide is primarily related to an anomalous solvent dielectric reorganization on the basis of the following: (i) The substitution has no detectable effect on the fine

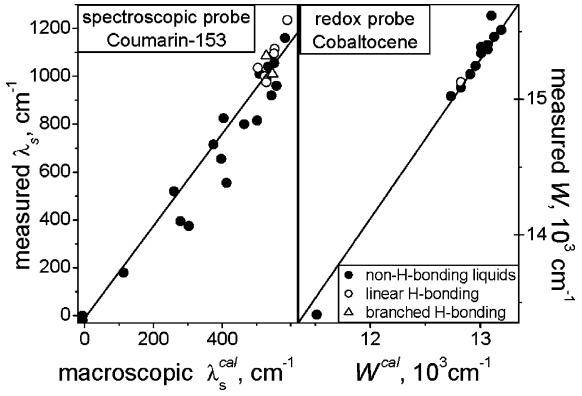

Figure 4. Measured dielectric response energies in different solvents vs macroscopic energies calculated within the dielectric continuum model similarly to PF (Figure 2). (Left) Solvent reorganization energy λ_s of dye coumarin-153 (data of ref 11) with dipolar-like electron density redistribution (dipolar component ~4.5 D). The straight line is a fit. Aromatic solvents and solvents with bulky nonpolar chains are omitted from the original data, because these solvents are suspected to be prone to "nonideal" (specific) interactions with the aromatic solute C153. Also omitted are nonpolar solvents that have high quadrupolar moments and may not obey the macroscopic model.[54] (Right) Energy of the total dielectric response W of the redox probe cobaltocene with ionic-like charge redistribution (the data adapted[131] from ref 1).

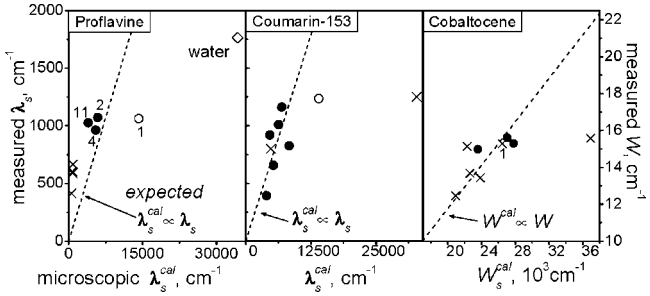

Figure 5. Measured solvent response energies of dielectric probes in several solvents vs microscopic response energies λ_s^{cal} and W^{cal} calculated within nonlocal smeared-charge model. Solvents are numbered according to Figure 2: (1) methanol, (2) acetonitrile, (4) DMSO, (11) acetone. (×) Cross symbols mark solvents whose "measured" energies were generated on the basis of the macroscopic predictions.[132] λ_s^{cal} and W^{cal} are calculated from bulk dielectric response functions $\chi(k)$ of the solvents and charge redistribution $\Delta\rho(k)$ of the probes (Figure 6b,c). Although the microscopic model cannot predict exact values of λ_s and W due to intrinsic uncertainties of the model parameters, we expect that λ_s^{cal} and W^{cal} should be proportional to λ_s and W. A few percentage point changes of measured values of λ_s and W with solvent vs tens to hundreds of percentage point changes of λ_s^{cal} and W^{cal} suggests that the model does not correlate with the data (Table 1).

intramolecular vibronic structure of the absorption and emission spectra of PF in the studied solvents, indicating that reorganization of the PF molecule and PF−solvent hydrogen bonds contributes little to the isotope effect on λ (see Supporting Information, Figure 4S). (ii) The same increase in λ is observed in both non- and linear H-bonding nonanomalous solvents (e.g., DMSO and methanol, see Figure 3). (iii) This ~5 cm^{-1} increase in λ seems to be related to the intramolecular reorganization energy, as is the case with non-H-bonding solvents such as DMSO, which are not subject to substitution, so the solvent should not contribute to the isotope effect on λ.

No anomaly was observed in the pressure dependence of the reorganization energy in the 0−2 kbar range. The dependence was weak and linear (the slopes $d\lambda/dP \approx 1$, 9, and 3 ± 5 cm^{-1}/kbar in water, methanol, and acetonitrile, respectively, were small compared to ~1000 cm^{-1} solvent reorganization energies).

4.2. Dielectric Calculations. *Macroscopic Dielectric Continuum Model.* The model reproduces measured dielectric response energies without adjustable parameters not only for PF but also for two other dielectric probes in nonanomalous solvents (Table 1, Figures 2 and 4). The ratio $x = \lambda_s^{cal}/\lambda_s$ of TDDFT-calculated and measured response energies is close to unit to within a small uncertainty of ~20% (somewhat lower $\bar{x}$ for C153 is probably due to systematically overestimated experimental λ_s[20]). This uncertainty is associated with intrinsic uncertainties in the definition of the solute/solvent interface (scaling factor α) at the microscopic scale and uncertainty of quantum chemical calculations (e.g., CIS, believed to be less accurate than TDDFT quantum chemical scheme, predicts 1.4 times higher λ_s^{cal} for PF and C153). But these uncertainties have almost no effect on the functional dependence of $\lambda_s(\epsilon_{op}, \epsilon_{st})$ and $W(\epsilon_{st})$ on the solvent dielectric constants and related solvent-to-solvent variation in x, $\Delta x/\bar{x}$ ($\Delta x \equiv \max\{x_i\} - \min\{x_i\}$ is the maximal variation of x within a given set of solvents).

The model predicts weak (compared to absolute values of $\lambda_s \approx 1000$ cm^{-1}) pressure ($d\lambda_s^{cal}/dP \approx 25$ cm^{-1}/kbar) and temperature ($d\lambda_s^{cal}/dT \approx 0.2$ cm^{-1}/K) dependences for PF which are in reasonable agreement with experimental values of $d\lambda/dP \approx 5$ cm^{-1}/kbar and $d\lambda/dT \approx 1 \pm 0.6$ cm^{-1}/K (Table 2). Small discrepancies between measured and calculated derivatives may be associated with small systematic errors in experimental λ values and/or with solvent molecules forming hydrogen bonds with PF whose small contribution to λ_s (~10%, Section 3.5) may have different pressure or temperature dependence.

If the cavity effect is neglected, the model still produces reasonable absolute values of the response energies and slightly poorer solvent variation $\Delta x/\bar{x}$ (smeared charge model with macroscopic $\chi(k) = \chi(0)$, Table 1).

Nonlocal Smeared Charge Model. This model produces no agreement with the data for either anomalous or nonanomalous solvents at reasonable values of the adjustable model parameters (Table 1, Figure 5). Even if the model inputs are artificially modified with adjustable parameters beyond the reasonable range of values, the model cannot describe dielectric response energies and their solvent dependence at the same time.

Specifically, without the adjustable parameters ($a = b = 0$, eq 4), the model overestimates response energies for nonanomalous solvents by more than an order of magnitude, $x = \lambda_s^{cal}/\lambda_s \gg 1$. More important, solvent-to-solvent variation in x is also too large, $\Delta x/\bar{x} \approx 1$.

Reasonable $\Delta x/\bar{x}$ (but still higher than for DCM without any cavity) can be achieved only at unreasonable values of parameters a and b (e.g., when the size of the smeared $\Delta\rho(\mathbf{r})$ exceeds the molecular size by an order of magnitude ($a = 4-9$ Å) or when the nonlocal part of the response functions, $\chi(k) - \chi(0)$, is by $b = 10-100$ times lower than predicted by computer simulations). However, then the ratio x becomes too small, that is, the model underestimates the response energies by 1−2 orders of magnitude. (The lower and the upper bounds of these ranges correspond to Cp_2Co and PF, respectively, with C153 in the middle.)

This model fails to describe the anomalous water solvent as well. It overestimates λ_s(water) by a factor of 20 for PF (Figure 5). The measured value can be reproduced at $\chi(k) - \chi(0)$ reduced $b \approx 100$ fold, as discussed already. Although unavailable from simulations, $\chi(k)$ of formamide and glycerol should be qualitatively similar to $\chi(k)$ of methanol and water (Figure 6a), and the model should still fail.

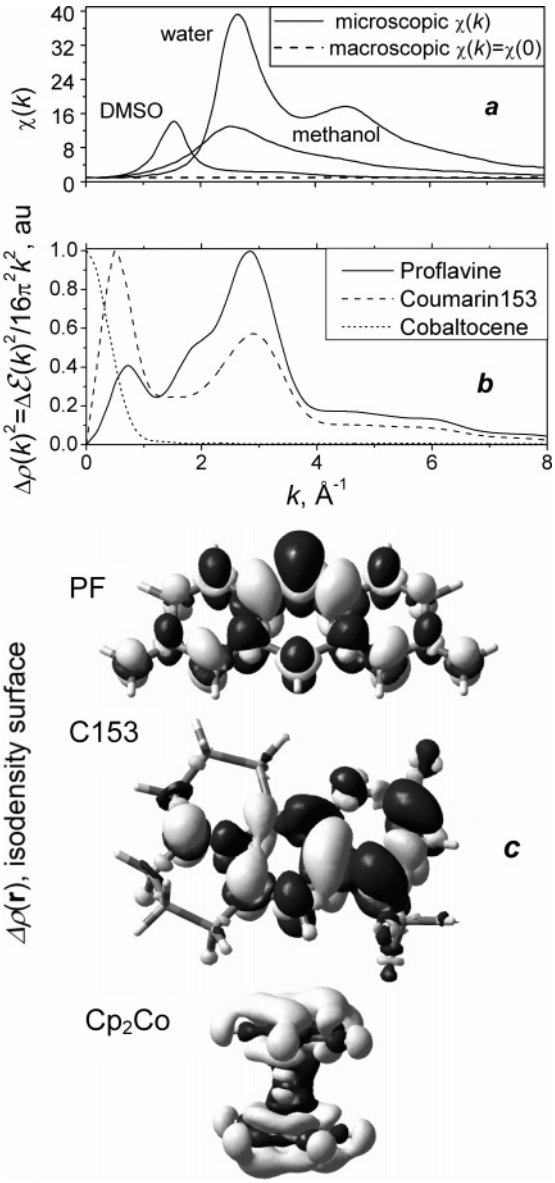

Figure 6. (a) Fourier transformed dielectric response function $\chi(k) = 1 - 1/\epsilon(k)$ of bulk dipolar solvents obtained from computer simulations or theory of dipolar liquids (data from ref 58). For dipolar solvents, the peaks in $\chi(k)$ were attributed primarily to intermolecular solvent−solvent correlations. For all dipolar solvents studied in such simulations, $\chi(k)$ substantially exceeded its macroscopic limit $\chi(0) = \chi \leq 1$. (b) Fourier transform $\Delta\rho(k)$ of charge redistribution $\Delta\rho(\mathbf{r})$ of the dielectric probes proflavine, coumarin-153, and cobaltocene (eq 3). Within the nonlocal theory (eqs 2 and 3),[55,56] a large contribution to $\Delta\rho(k)$ of high $k > 0.5$ Å^{-1} (where $\chi(k) > 1$) leads to strong deviations of energies of the solvent dielectric response from macroscopic predictions based on $\chi(0)$. More important, the unique structure and $\chi(k)$ of each solvent leads to strong solvent-to-solvent variation of the response energies predicted by the existing nonlocal theories. (c) Electron density redistributions $\Delta\rho(\mathbf{r})$'s of the probes. Isodensity surfaces at $\Delta\rho = \pm 0.0015$ atomic units shown in dark and light shades were obtained from CIS/6-31G(d,p)/nonequilibrium-IEFPCM and B3LYP/6-31+G-(d,p) ab initio calculations.

The Lorentzian approximation of the response function[55,82−84,89] produced no sensible results either. Although the approximation reproduced satisfactory solvent variation ($\Delta x/\bar{x}$ was similar to the DCM smeared charge model, Table 1), it required unrealistic assumptions: To fit the measured response energies for the same solvent (nonanomalous or anomalous), the polarization correlation length l of the same solvent should differ by 20 times for different probes ($l \approx 2$ Å for Cp_2Co and $l \approx 0.1$ Å for PF and C153). Furthermore, such $l \approx 0.1$ Å should be unphysically short.

We verified that the model fails qualitatively regardless of the choice of smearing function, uncertainties in approximations of charge redistributions, and the origin of the simulated $\chi(k)$ (e.g., $\chi(k)$ derived from dipole−dipole[86,107] instead of charge−charge spatial correlations).

5. Discussion

5.1. Static Microscopic Dielectric Response of Most Solvents Is Described by Macroscopic Dielectric Constants without Adjustable Parameters. In this study, we analyzed energies of the static dielectric response of dipolar solvents to charge redistribution in three different solutes, because this kind of energy is expected to be less sensitive to nondielectric contributions from specific solute−solvent interactions than other solvation-related energies (Section 2.2). Namely, we spectroscopicaly evaluated the solvent reorganization energy λ_s in response to electron density redistribution in a fluorescent probe, proflavine (PF). The quadrupolar-like charge redistribution of PF occurs on microscopic $\pi/k = 1-7$ Å length scale (the dominating contribution is at $\pi/k = 1-2.5$ Å) comparable with solvent molecular size (Figures 1 and 6). Nevertheless, we found that the solvent dependence of λ_s for most dipolar solvents (with a few interesting exceptions to be discussed) is described by macroscopic dielectric constants within the dielectric continuum model (DCM) (Figure 2). Our auxiliary studies indicated that specific dye−solvent interactions contribute little to such dependence.

The agreement for such a large number of solvents is not likely to be a coincidence, and it is not a unique feature of our spectroscopic probe. Similar analysis shows that DCM also describes the data[11] for another spectroscopic probe, coumarin-153 (C153) with dipolar-like charge redistribution at $\pi/k = 1-25$ Å length scale (the dominating contribution is at 2.5−25 Å)[108] (Figure 6b). Like PF, C153 does not seem to have any significant reorganization of specific solute−solvent interactions, as confirmed by our data on the solvent isotope effect (Supporting Information Figure 4S) and by simulations.[45]

Furthermore, DCM was demonstrated to work well for a physically different process with ionic-like charge redistribution at >5 Å length scale[1,2] (Figure 6b). The energy of the dielectric response was measured via the difference of the redox potentials of two successive redox reactions

$$A^z \overset{+1e}{\longleftrightarrow} A^{z-1} \overset{+1e}{\longleftrightarrow} A^{z-2}$$

for complex metal ions of several sizes (e.g., cobaltocene, Cp_2Co). Such measurements for these rather big (radii ≈ 4 Å), low-charge ($z = \pm 1, 0$) ions were designed to reduce the contribution from nonlinear effects, specific solute−solvent interactions, solvent pre-existing potential, and other effects obscuring the linear dielectric response.[1,2]

In addition, computer simulations of solutes such as C153 in molecular solvents also showed reasonable agreement of simulated λ_s values with DCM.[26,43,45]

Substantial deviations from DCM were observed mostly when specific solute−solvent interactions were significant.[1,4,10,17,49,109] It appears that these deviations are primarily related to probe-specific effects rather than to intrinsic features of the microscopic dielectric response of dipolar solvents. For probes and experimental methods with weak contributions from specific solute−solvent interactions, only minor deviations were reported. We

find the deviations to be even smaller if DCM analysis is coupled with quantum chemical calculations implementing a more rigorous DCM approach, detailed molecular cavity, and electronic polarizability of solutes.[110] This is the case with PF, C153, Cp_2Co (shown in Figures 2, 4, and Table 1) and some other systems[3,50] (not shown). An account of some of these factors within time- or frequency-resolved generalizations of the DCM model was also shown to improve the description of solvation energetics of several solutes.[52,53,111]

Deviations from DCM were also predicted to be due to translational (density) response of solvent molecules on the basis of the approximate decoupling of contributions from translational and rotational motions within certain molecular liquid theories.[112] However, such deviations do not seem to be significant at least in our case. (i) Indeed, an incorrect sign of temperature dependence $d\lambda/dT$ of the reorganization energy λ in nonanomalous dipolar solvents predicted by the macroscopic model for a dipolar spectroscopic probe was used as evidence.[8,9] To the contrary, our calculations predict reasonable $d\lambda/dT$ values measured for our probe in most dipolar solvents to within the estimated uncertainties of spectra processing (associated, for example, with temperature-dependent spectral band shape, cf. Table 2). The apparent discrepancy may be due to several factors neglected in the previous analysis[8,9] (i.e., solute polarizability, which may change the sign of the predicted $d\lambda/dT$ value,[113] the systematic uncertainties and/or other contributions obscuring linear dielectric response). (ii) Furthermore, one might expect the translational contribution to be sensitive to the effect of pressure on solvent density,[112] which is not observed for our probe whose negligible pressure dependence is consistent with macroscopic predictions. (iii) Finally, in linear response to the electric field, solvent density changes should arise from asymmetry of the solvent molecule,[114] which is different for different molecular solvents. As a result, dielectric response energies of solvents with significant density changes should deviate from the macroscopic prediction to a different extent, which is not observed for the dielectric probes analyzed here. Further analysis will help to improve the understanding of translational response which is beyond the scope of this work.

5.2. Water, Formamide, and Glycerol Exhibit Dielectric Anomaly. Notable exceptions are branched H-bonding solvents, which exhibit entirely different behavior. Particularly strong deviations are observed for PF in water, formamide, and glycerol whose solvent reorganization energy cannot be explained even qualitatively by DCM (Figure 2). One would have to assume impossible negative values of ϵ_{st} in order to fit abnormally high λ_s values of these solvents. Furthermore, λ_s in these solvents exhibits inverted temperature dependence, solvent isotope (Figure 6) and cosolvent[106] effects that are not observed in other solvents.

We attribute this behavior to anomalous dielectric properties of water, formamide, and glycerol rather than to probe- or solvent-specific effects. Such an interpretation is based on our extensive auxiliary experiments and quantum chemical calculations (Section 3 and Supporting Information) suggesting that: (i) The anomaly cannot be explained by specific probe−solvent interactions. Indeed, PF donates hydrogen bonds to all dipolar solvents, but only a few solvents exhibit the anomaly. In addition, PF can accept a weak H-bond from H-bonding solvents. The accepted bond is expected to be weak, because PF is a cation (low H-bond energy of ∼1 kcal/mol and long bond length of ∼3.1 Å were calculated, Section 1.2S in Supporting Information). Such a bond would be expected in both linear and branched H-bonding solvents, which have similar H-bond-donor strength. However, such a bond results in slightly decreased reorganization energy in linear H-bonding solvents compared to non-H-bonding solvents, Figure 2. A small effect of the accepted H-bond is also predicted by quantum chemical calculations (Section 1.7S in Supporting Information). Furthermore, the lack of correlation between the reorganization energy and solvent H-bond-donor strength[115] also suggests that accepting an H-bond is not responsible for the anomaly. If specific PF−solvent interactions were responsible for the anomalous reorganization, one would expect to see their manifestation in other molecular properties such as transition dipole moment, fluorescence quantum yield, isotope effect on the fine intramolecular vibronic structure of the absorption and emission spectra, vibrational spectra, and so on, but this is not observed. The lack of observed effects is consistent with quantum chemical calculations of PF in supermolecular complexes with solvent molecules imitating various kinds of specific PF−solvent interactions, which indicate no significant influence of complex formation on the parameters of PF structure that causes reorganization of the PF−solvent system upon excitation. (ii) The anomaly is not a unique property of the probe−solvent interface. Anomalously high reorganization energy and anomalous cosolvent effects were also observed for the dye bound inside a water-soluble, globular protein away from direct contact with water (also indicating that specific PF−solvent interactions cannot explain the anomaly).[106,116] When the dye−protein complex was dehydrated and covered by only 1−2 monolayers of water, the anomaly disappeared,[116] suggesting that the anomaly is a property of the liquid rather than of adsorbed molecules of water. In addition, the anomaly appears to be present in acridine orange, a methylated analogue of PF whose first solvation shell is different.[117] (iii) The anomaly is not associated with (a) the size of solvent molecule and (b) lower solvent density and its fluctuations near the probe. In particular, (a) formamide, methanol, and acetonitrile have similar sizes, but only formamide exhibits the anomaly; (b) λ values in water, methanol, and acetonitrile solvents are virtually insensitive to pressure and, therefore, to solvent density and its fluctuations.

An empirical insight into the potential origin of the anomaly can be gained from differences between anomalous and nonanomalous solvents. The most important one is the ability of anomalous solvents to form 3D hydrogen-bond networks suggesting that the anomaly is somehow related to solvent structure. This is supported by the observed cosolvent[106] and solvent isotope effects (Figure 3). Indeed, cosolvents are known to disrupt H-bond network in water, and they destroy the anomaly; deuteration is believed to strengthen hydrogen bonds and their networks, and the H → D substitution enhances the anomaly in D_2O and deuterated formamide. However, not all structured solvents exhibit the anomaly. For example, we observed substantially smaller deviations in the propane diols and ethylene glycol despite their ability to form 3D H-bond networks. Furthermore, we observed no anomaly in non- and linear-H-bonding solvents which are structured at the molecular scale (see following text). Thus, the presence of solvent structure seems to be a necessary but not sufficient condition for the anomaly.

Note that various solvation-related properties of branched solvents were previously reported to be anomalous. However, anomalous response energies were usually observed in both linear and branched H-bonding solvents and, thus, appear to be a result of probe−solvent H-bonds.

5.3. Measured Response of Nonanomalous and Anomalous Solvents Indicates Nontrivial Properties of Solvent Response

Tensor. In summary, our analysis reveals a nontrivial relationship between static microscopic dielectric response and the molecular-scale structure of dipolar solvents. Measured response energies of most dipolar solvents, non-hydrogen-bonding and linear hydrogen-bonding, behave as if these solvents were unstructured (local) macroscopic dielectrics even at the atomic scale, in contrast to predictions of seemingly more appropriate nonlocal dielectric models that account for molecular-scale solvent structure (Figures 2, 4, and Table 1). A few branched hydrogen-bonding solvents, whose physical chemical properties are similar to the macroscopic-like solvents, show anomalous, nonmacroscopic response somehow related to their intermolecular structure (Figures 2 and 3). But the data for anomalous solvents disagree with the existing microscopic nonlocal models (Figures 2 and 5). These models fail to describe not only the correct order of magnitude of the measured dielectric response energies but also their solvent-to-solvent variation at any values of adjustable parameters introduced in an attempt to improve the predictions.

Here, we chose simplified continuum-like models. They are not as accurate and detailed as full microscopic calculations (e.g., simulations of particular systems), but simulations do not easily yield the underlying physics. The advantage of data analysis within the chosen models is that they implement rigorous linear response theory under different assumptions (Section 2.2), and an insight into the response−structure relationship is gained as a result.

Within the linear response theory, solvent response is determined by the product of the electric field $\Delta\mathcal{E}(\mathbf{r})$ produced by solute charge redistribution and the solvent dielectric response tensor $\chi_{\alpha\beta}(\mathbf{r}, \mathbf{r}')$ related to solvent structure (spatial correlator of polarization fluctuations) via the fluctuation dissipation theorem.[55,56,82−84] Static response of molecular solvents is continuum-like, because solvent molecules have enough time to sample space around the solute by translational motions. Nevertheless, such a continuum-like response retains information about microscopic solvent structure due to short-range correlations between solvent dipoles[34,35,37,55,56,76,77,118] (Section 2.2). The advantage of this theory is its broad applicability. (It applies to arbitrary configurations of weak electric fields and dielectric geometries of continuous or discrete dielectrics at both microscopic and macroscopic length scales and accounts for both rotational and translational degrees of freedom of molecular dielectric.) The only drawback is that the general form of the response−structure relationship as well as response tensors of particular solute−solvent systems are still not known.[76] Thus, the existing implementations of the response theory rely on the limited available knowledge and model approximations for $\chi_{\alpha\beta}(\mathbf{r}, \mathbf{r}')$.

Specifically, the macroscopic model, assuming that the solvent has no spatial structure at the characteristic length scales of spatial variation of the solute electric field, approximates $\chi_{\alpha\beta}(\mathbf{r}, \mathbf{r}')$ by the local function $\chi\delta_{\alpha\beta}\delta(\mathbf{r} - \mathbf{r}')$ determined by the macroscopic dielectric constant ϵ_{st} ($\chi = 1 - 1/\epsilon_{st}$). Visual inspection of electron density redistributions of the analyzed dielectric probes (Figure 6c) indicates a violation of this macroscopic assumption, because the electric field imposed by such redistributions on the surrounding solvent exhibit rapid spatial variation on the length scale of solvent molecular size. Then, solvent response should be described by the nonlocal response function $\chi_{\alpha\beta}(\mathbf{r}, \mathbf{r}') \neq \chi\delta_{\alpha\beta}\delta(\mathbf{r} - \mathbf{r}')$.

Properties of $\chi_{\alpha\beta}(\mathbf{r}, \mathbf{r}')$ far from the solute, where it coincides with the response tensor of the bulk isotropic solvent $\chi_{\alpha\beta}(\mathbf{r} - \mathbf{r}')$, were studied by several independent methods. Molecular theories,[26,27,36,58,60] simulations,[27,36,38,58−60] and neutron scattering[60] of bulk liquids suggested that intermolecular ordering of dipolar solvents leads to high peaks in Fourier transform $\chi(k)$ of the response function $\chi(\mathbf{r} - \mathbf{r}')$ (Figure 6a). Wave vector k-dependence of $\chi(k)$ means that the response functions are strongly nonlocal at $\pi/k \approx 1-6$ Å length scales (i.e., the length scales of electric field $\Delta\mathcal{E}$ produced by charge redistribution $\Delta\rho$ in the analyzed probes) (Figure 6b,c).

Within the most popular nonlocal smeared charge model assuming that the bulk function $\chi(\mathbf{r} - \mathbf{r}')$ is not perturbed by solute, the resulting overlap between solute electric field $\Delta\mathcal{E}(\mathbf{k})$ and peaks in $\chi(k)$ should produce a resonant dielectric response with anomalously high energy (eqs 2 and 3). More important, because spatial structure and position and height of the related peaks are quite different for different solvents, the response energy should dramatically vary from solvent to solvent, which is not observed (Figure 5, Table 1). To the contrary, the measured response energies of most dipolar solvents conform to the local macroscopic model (Figures 2, 4, and Table 1) whose underlying assumption of the absence of nonlocal spatial solvent structure is strongly violated (Figure 6).

This illustration of nonlocal paradox is based on the nonlocal model neglecting the exclusion of solvent from the solute cavity. However, the paradox cannot be easily explained by the presence of the solute cavity:

First, our estimates indicate that other nonlocal models that account for the solute cavity effect do not substantially modify these predictions and cannot describe the data either.[119−121] All existing nonlocal models are based on heuristic relationships between $\chi_{\alpha\beta}(\mathbf{r}, \mathbf{r}')$ and bulk response functions $\chi(\mathbf{r} - \mathbf{r}')$ which have been proposed or borrowed from plasma physics[55,56] (Section 2.2). Application of these approximations to dipolar materials has never been justified, and apparently, they do not capture the physics of the solute cavity effect appropriately.

Second, near the solute cavity, spatial correlations between the surrounding solvent molecules may be perturbed, but these correlations cannot be completely eliminated. (Simulations indicate the presence of correlations[42] and neutron scattering even suggests that correlations in the vicinity of solutes and in the solvent bulk are similar.[122]) Thus, $\chi_{\alpha\beta}(\mathbf{r}, \mathbf{r}')$ near the solute should still be essentially nonlocal and resonant on the length scales of electric fields $\Delta\mathcal{E}$ produced by the analyzed probes. An opinion exists that occasionally observed macroscopic-like behavior can be explained by accidental cancellations of molecular effects (e.g., cancellation of the molecular correlations and ambiguous proximity of the solute cavity boundary to the solute charge). However, these correlations (and other molecular effects) should still be quite different for different solvents. Thus, it is difficult to explain the macroscopic-like response observed in several solute−solvent systems by accidental cancellations, unless the response tensors of most dipolar solvents have some common nontrivial property, which is not yet understood.

5.4. Hypothesis. We believe that the electric field produced by charges located inside the solute cavity or outside the solvent may not be coupled to isotropic nonlocal bulk modes of solvent polarization fluctuations and may not elicit a resonant dielectric response. Unless solvent structure at the solute surface is substantially different from the bulk, the dielectric response to solute charges may be macroscopic-like despite the high peak in bulk response function $\chi(k)$. (In other words, solvent polarization induced by cavity charges may formally comply with the local relationship $4\pi\Delta\mathbf{P} = \chi\Delta\mathbf{D}$, despite essentially nonlocal response function $\chi_{\alpha\beta}(\mathbf{r}, \mathbf{r}') \neq \chi\delta_{\alpha\beta}\delta(\mathbf{r} - \mathbf{r}')$, to be shown elsewhere.)

The origin of the anomalous dielectric response of branched hydrogen-bonding solvents, water, formamide, and glycerol, remains to be understood. The following hints might help in understanding the anomaly. By the fluctuation dissipation theorem, the anomalous response indicates the presence of anomalously strong modes of solvent polarization fluctuations that are coupled to an electric field of charge redistribution inside the probe. Our results indicate that these modes are somehow related to fluctuating intermolecular structure of the solvent adjacent to the hydrophobic-like area of the probe's surface (i.e., area that is free of probe−solvent H-bonds). Interestingly, molecules of branched H-bonding solvents (e.g., water and formamide) exhibit strongly anisotropic packing at hydrophobic and liquid/air interfaces in order to minimize the loss of H-bonds they would have in the bulk,[122−129] while nonanomalous solvents (e.g., methanol) exhibit qualitatively different interfacial organization.[125] Thus, we cannot rule out that similar packing at the probe's surface may create a spatial correlator of polarization fluctuations which is not only different from that of nonanomalous solvents but also has a new superficial pattern of polarization fluctuations near the probe. Such a polarization pattern may resonate with charge redistribution inside the probe, if the two patterns match. The resulting surface resonance may contribute to the anomalous response observed for our probe,[130] a hydrophobic molecule whose pattern of charge redistribution rapidly varies along the molecular plane (Figures 1 and 6).

6. Conclusions

Dielectric response energies of most dipolar solvents to charge redistribution in molecular solutes do not conform to simple expectations based on the nonlocal spatial structure predicted by computer simulations of bulk solvents. Instead, most solvents respond as if they were unstructured local dielectrics described by their macroscopic dielectric constants even at the microscopic scale. To resolve this apparent discrepancy, we suggest that resonant bulk modes of polarization fluctuations predicted by simulations do not interact with the charge redistribution located inside a solute cavity (or outside the solvent).

Water, formamide, and glycerol exhibit an anomalous dielectric response somehow related to intermolecular solvent structure. Such a response indicates the existence of anomalously strong polarization fluctuations that interact with the charge redistribution of our solute. The origin of the anomaly remains to be understood.

Acknowledgment. I am indebted to L. I. Krishtalik and S. Leikin for stimulating discussions of this work. I thank J. Knutson for giving access to the SLM8000 spectrometer.

Supporting Information Available: Details on auxiliary experiments and quantum chemical calculations used for proflavine characterization. Tabulated and plotted data on measured and calculated reorganization energies of proflavine. This material is available free of charge via the Internet at http://pubs.acs.org.

References and Notes

(1) Krishtalik, L. I.; Alpatova, N. M.; Ovsyannikova, E. V. *Electrochim. Acta* **1991**, *36*, 435−445. Bunakova, L. V.; Topolev, V. V.; Khanova, L. A.; Krishtalik, L. I. *Elektrokhimiya* **2004**, *40*, 913.

(2) Alpatova, N. M.; Ovsyannikova, E. V.; Krishtalik, L. I. *Elektrokhimiya* **1991**, *27*, 823.

(3) Brunschwig, B. S.; Eherenson, S.; Sutin, N. *J. Phys. Chem.* **1986**, *90*, 3657.

(4) Walker, G. C.; Akesson, E.; Johnson, A. E.; Levinger, N. E.; Barbara, P. F. *J. Phys. Chem.* **1992**, *96*, 3728.

(5) Hupp, J. T.; Dong, Y. H.; Blackbourn, R. L.; Lu, H. *J. Phys. Chem.* **1993**, *97*, 3278.

(6) Cortes, J.; Heitele, H.; Jortner, J. *J. Phys. Chem.* **1994**, *98*, 2527.

(7) Kapturkiewicz, A.; Herbich, J.; Karpiuk, J.; Nowacki, J. *J. Phys. Chem. A* **1997**, *101*, 2332.

(8) Vath, P.; Zimmt, M. B. *J. Phys. Chem. A* **2000**, *104*, 2626.

(9) Vath, P.; Zimmt, M. B.; Matyushov, D. V.; Voth, G. A. *J. Phys. Chem. B* **1999**, *103*, 9130.

(10) Kjaer, A. M.; Ulstrup, J. *J. Am. Chem. Soc.* **1987**, *109*, 1934.

(11) Reynolds, L.; Gardecki, J. A.; Frankland, S. J. V.; Horng, M. L.; Maroncelli, M. *J. Phys. Chem.* **1996**, *100*, 10337.

(12) Horng, M. L.; Gardecki, J. A.; Papazyan, A.; Maroncelli, M. *J. Phys. Chem.* **1995**, *99*, 17311.

(13) Nishiyama, K.; Okada, T. *J. Phys. Chem. A* **1997**, *101*, 5729.

(14) Nishiyama, K.; Hirata, F.; Okada, T. *J. Mol. Liq.* **2001**, *90*, 251.

(15) Myers, A. B. *Chem. Rev.* **1996**, *96*, 911.

(16) Zong, Y. P.; McHale, J. L. *J. Chem. Phys.* **1997**, *106*, 4963.

(17) Jordanides, X. J.; Lang, M. J.; Song, X. Y.; Fleming, G. R. *J. Phys. Chem. B* **1999**, *103*, 7995.

(18) Matyushov, D. V.; Schmid, R.; Ladanyi, B. M. *J. Phys. Chem. B* **1997**, *101*, 1035.

(19) Matyushov, D. V.; Voth, G. A. *J. Chem. Phys.* **1999**, *111*, 3630.

(20) Matyushov, D. V.; Newton, M. D. *J. Phys. Chem. A* **2001**, *105*, 8516.

(21) Maroncelli, M. *J. Chem. Phys.* **1997**, *106*, 1545.

(22) Kornyshev, A. A.; Nitzan, A. *Z. Phys. Chem.* **2001**, *215*, 701.

(23) Rocchia, W.; Alexov, E.; Honig, B. *J. Phys. Chem. B* **2001**, *105*, 6507.

(24) Liu, Y.-P.; Newton, M. D. *J. Phys. Chem.* **1994**, *98*, 7162−7169; *J. Phys. Chem.* **1995**, *99*, 12382−12386.

(25) Marcus, R. A. *J. Phys. Chem.* **1994**, *98*, 7170.

(26) Perng, B. C.; Newton, M. D.; Raineri, F. O.; Friedman, H. L. *J. Chem. Phys.* **1996**, *104*, 7177.

(27) Perng, B. C.; Newton, M. D.; Raineri, F. O.; Friedman, H. L. *J. Chem. Phys.* **1996**, *104*, 7153.

(28) Dogonadze, R. R.; Itskovich, E. M.; Kuznetsov, A. M.; Vorotyntsev, M. A. *J. Phys. Chem.* **1975**, *79*, 2827.

(29) Ishida, T.; Hirata, F.; Kato, S. *J. Chem. Phys.* **1999**, *110*, 11423.

(30) Basilevsky, M. V.; Parsons, D. F. *J. Chem. Phys.* **1998**, *108*, 9114.

(31) Cramer, C. J.; Truhlar, D. G. *Chem. Rev.* **1999**, *99*, 2161.

(32) Chan, D. Y. C.; Mitchell, D. J.; Ninham, B. W. *J. Chem. Phys.* **1979**, *70*, 2946.

(33) van der Zwan, G.; Hynes, J. T. *J. Phys. Chem.* **1985**, *89*, 4181.

(34) Bagchi, B.; Chandra, A. *Phys. Rev. Lett.* **1990**, *64*, 455.

(35) Chandra, A.; Bagchi, B. *J. Phys. Chem.* **1989**, *93*, 6996.

(36) Chandra, A.; Bagchi, B. *J. Chem. Phys.* **1989**, *90*, 1832.

(37) Chandra, A.; Bagchi, B. *J. Chem. Phys.* **1989**, *91*, 7181.

(38) Pollock, E. L.; Alder, B. J. *Phys. Rev. Lett.* **1981**, *46*, 950.

(39) Hummer, G.; Pratt, L. R.; Garcia, A. E. *J. Phys. Chem. A* **1998**, *102*, 7885.

(40) Lobaugh, J.; Rossky, P. J. *J. Phys. Chem. A* **2000**, *104*, 899.

(41) Ishida, T.; Rossky, P. J. *J. Phys. Chem. A* **2001**, *105*, 558.

(42) Ladanyi, B. M.; Maroncelli, M. *J. Chem. Phys.* **1998**, *109*, 3204.

(43) Mente, S. R.; Maroncelli, M. *J. Phys. Chem. B* **1999**, *103*, 7704.

(44) Cichos, F.; Brown, R.; Bopp, P. A. *J. Chem. Phys.* **2001**, *114*, 6834.

(45) Kumar, P. V.; Maroncelli, M. *J. Chem. Phys.* **1995**, *103*, 3038.

(46) Li, J.; Cramer, C. J.; Truhlar, D. G. *Int. J. Quantum Chem.* **2000**, *77*, 264.

(47) Tran, V.; Schwartz, B. J. *J. Phys. Chem. B* **1999**, *103*, 5570.

(48) Aherne, D.; Tran, V.; Schwartz, B. J. *J. Phys. Chem. B* **2000**, *104*, 5382.

(49) Krishtalik, L. I.; Alpatova, N. M.; Ovsyannikova, E. V. *Elektrokhimiya* **1995**, *31*, 802.

(50) Hupp, J. T.; Weydert, J. *Inorg. Chem.* **1987**, *26*, 2657.

(51) Time-dependent dielectric properties are more complex, because they are determined by a larger number of statistical variables, velocities, and coordinates (in other words, by temporal and spatial dispersion of solvent), while static properties are determined by coordinates only (spatial dispersion). Abrikosov, A. A.; Gorkov, I. E.; Dzyaloshinski, I. E. *Methods of quantum field theory in statistical physics*; Silverman R. A., Ed; Prentice Hall: Englewood Cliffs, NJ, 1963. References 75 and 76.

(52) Hsu, C. P.; Georgievskii, Y.; Marcus, R. A. *J. Phys. Chem. A* **1998**, *102*, 2658.

(53) Song, X. Y.; Chandler, D. *J. Chem. Phys.* **1998**, *108*, 2594.

(54) Significant deviations from the macroscopic model observed for quadrupolar solvents[11,26] are not surprising, because the model was developed for dipolar materials only.

(55) Kornyshev, A. A. In *The Chemical Physics of Solvation*; Dogonadze, R. R., Kalman, E., Kornyshev, A. A., Ulstrup, J., Eds; Elsevier: Amsterdam, 1985; p 77.

(56) Kornyshev, A. A.; Vorotyntsev, M. A. *Electrostatics of media with spatial dispersion*; Nauka: Moscow, 1993.

(57) Raineri, F. O.; Friedman, H. L. *Adv. Chem. Phys.* **1999**, *107*, 81.

(58) Raineri, F. O.; Perng, B. C.; Friedman, H. L. *Electrochim. Acta* **1997**, *42*, 2749.
(59) Ladanyi, B. M.; Skaf, M. S. *Annu. Rev. Phys. Chem.* **1993**, *44*, 335.
(60) Bopp, P. A.; Kornyshev, A. A.; Sutmann, G. *Phys. Rev. Lett.* **1996**, *76*, 1280.
(61) Mertz, E. L.; Tikhomirov, V. A.; Krishtalik, L. I. *J. Phys. Chem. A* **1997**, *101*, 3433.
(62) In our previous work,[61] we studied the same monocationic form of proflavine, which we mistakenly assigned to dication. This mistake was fixed in our subsequent publication.[116]
(63) Mataga, N.; Kaifu, Y.; Koizumi, M. *Bull. Chem. Soc. Jpn.* **1956**, *29*, 373.
(64) Marcus, R. A. *J. Chem. Phys.* **1963**, *38*, 1858.
(65) Mertz, E. L. *Chem. Phys. Lett.* **1996**, *262*, 27.
(66) Matyushov, D. V.; Schmid, R. *J. Chem. Phys.* **1995**, *103*, 2034.
(67) Matyushov, D. V. *Chem. Phys.* **1996**, *211*, 47.
(68) Krishtalik, L. I.; Kuznetsov, A. M.; Mertz, E. L. *Proteins* **1997**, *28*, 174.
(69) Aqvist, J.; Hansson, T. *J. Phys. Chem.* **1996**, *100*, 9512.
(70) Pratt, L. R.; Hummer, G.; Garcia, A. E. *Biophys. Chem.* **1994**, *51*, 147.
(71) Levy, R. M.; Belhadj, M.; Kitchen, D. B. *J. Chem. Phys.* **1991**, *95*, 3627.
(72) Simonson, T.; Perahia, D. *J. Am. Chem. Soc.* **1995**, *117*, 7987.
(73) Landau, L. D.; Lifschitz, E. M. *Statistical Physics, Part 1*; Nauka: Moscow, 1995.
(74) Landau, L. D.; Lifschitz, E. M. *Electrodynamics of Continuous Media*; Nauka: Moscow, 1992.
(75) Kubo, R.; Toda, M.; Hashitsume, N. *Statistical Physics II: Nonequilibrium Statistical Mechanics*; Springer-Verlag: Berlin, 1991.
(76) Dogonadze, R. R.; Kornyshev, A. A.; Kuznetsov, A. M.; Marasagishvili, T. A. *J. Phys.* (*Paris*) **1977**, *38*, C5−35.
(77) Bagchi, B.; Vijayadamodar, G. V. *J. Chem. Phys.* **1993**, *98*, 3351.
(78) Nienhuis, G.; Deutch, J. M. *J. Chem. Phys.* **1971**, *55*, 4213.
(79) Wertheim, M. S. *Annu. Rev. Phys. Chem.* **1979**, *30*, 471.
(80) Song, X. Y.; Chandler, D.; Marcus, R. A. *J. Phys. Chem.* **1996**, *100*, 11954.
(81) It is important to distinguish between requirements for macroscopic-like and continuum-like static dielectric responses. Within discrete (e.g., lattice) models usually used to describe solid or glassy dielectrics, these requirements are equivalent (negligible discreteness of dielectric is sufficient for macroscopic-like response, Papazyan A.; Warshel A. *J. Phys. Chem. B* **1997**, 101, 11254). In liquids, translational motions of solvent molecules result in a continuum-like response even at the molecular scale.[33−35,37] However, this is not sufficient for macroscopic-like response. For example, it was demonstrated using molecular liquid theories that macroscopic-like response is recovered when the diameter of the solute cavity with a charge or a dipole is much larger than the diameter of the solvent molecule.[32,35,77]
(82) Kornyshev, A. A. *Electrochim. Acta* **1981**, *26*, 1.
(83) Dogonadze, R. R.; Kornyshev, A. A. *J. Chem. Soc. Faraday Trans. 2* **1974**, *70*, 1121.
(84) Dogonadze, R. R.; Kornyshev, A. A.; Kuznetsov, A. M. *Teor. Mat. Fiz.* **1973**, *15*, 127.
(85) Kornyshev, A. A.; Leikin, S.; Sutmann, G. *Electrochim. Acta* **1997**, *42*, 849. Medvedev, I. G. *Electrochim. Acta* **2004**, *49*, 207.
(86) Bopp, P. A.; Kornyshev, A. A.; Sutmann, G. *J. Chem. Phys.* **1998**, *109*, 1939.
(87) Kornyshev, A. A.; Sutmann, G. *Electrochim. Acta* **1997**, *42*, 2801.
(88) Kornyshev, A. A.; Vorotyntsev, M. A. *J. Phys. C* **1979**, *12*, 4939.
(89) Vorotyntsev, M. A.; Kornyshev, A. A. *Zh. Eksp. Teor. Fiz.* **1980**, *78*, 1008.
(90) Frisch, M. J.; Trucks, G. W.; Schlegel, H. B.; Scuseria, G. E.; Robb, M. A.; Cheeseman, J. R.; Montgomery, J. A., Jr.; Vreven, T.; Kudin, K. N.; Burant, J. C.; Millam, J. M.; Iyengar, S. S.; Tomasi, J.; Barone, V.; Mennucci, B.; Cossi, M.; Scalmani, G.; Rega, N.; Petersson, G. A.; Nakatsuji, H.; Hada, M.; Ehara, M.; Toyota, K.; Fukuda, R.; Hasegawa, J.; Ishida, M.; Nakajima, T.; Honda, Y.; Kitao, O.; Nakai, H.; Klene, M.; Li, X.; Knox, J. E.; Hratchian, H. P.; Cross, J. B.; Adamo, C.; Jaramillo, J.; Gomperts, R.; Stratmann, R. E.; Yazyev, O.; Austin, A. J.; Cammi, R.; Pomelli, C.; Ochterski, J. W.; Ayala, P. Y.; Morokuma, K.; Voth, G. A.; Salvador, P.; Dannenberg, J. J.; Zakrzewski, V. G.; Dapprich, S.; Daniels, A. D.; Strain, M. C.; Farkas, O.; Malick, D. K.; Rabuck, A. D.; Raghavachari, K.; Foresman, J. B.; Ortiz, J. V.; Cui, Q.; Baboul, A. G.; Clifford, S.; Cioslowski, J.; Stefanov, B. B.; Liu, G.; Liashenko, A.; Piskorz, P.; Komaromi, I.; Martin, R. L.; Fox, D. J.; Keith, T.; Al-Laham, M. A.; Peng, C. Y.; Nanayakkara, A.; Challacombe, M.; Gill, P. M. W.; Johnson, B.; Chen, W.; Wong, M. W.; Gonzalez, C.; Pople, J. A. *Gaussian 03*, revision B.03; Gaussian, Inc.: Pittsburgh, PA, 2003.
(91) Casida, M. E.; Jamorski, C.; Casida, K. C.; Salahub, D. R. *J. Chem. Phys.* **1998**, *108*, 4439.
(92) Adamo, C.; Scuseria, G. E.; Barone, V. *J. Chem. Phys.* **1999**, *111*, 2889.
(93) Adamo, C.; Barone, V. *Chem. Phys. Lett.* **1999**, *314*, 152.
(94) Cave, R. J.; Burke, K.; Castner, E. W. *J. Phys. Chem. A* **2002**, *106*, 9294.
(95) Lee, C. T.; Yang, W. T.; Parr, R. G. *Phys. Rev. B* **1988**, *37*, 785.
(96) Becke, A. D. *J. Chem. Phys.* **1993**, *98*, 5648.
(97) Tretzel, J.; Schneider, F. W. *Chem. Phys. Lett.* **1978**, *59*, 514.
(98) Clarke, R. H.; HA, S. *Spectrochim. Acta A* **1985**, *41*, 1381.
(99) Hedberg, A. K.; Hedberg, L.; Hedberg, K. *J. Chem. Phys.* **1975**, *63*, 1262.
(100) Fey, N. *J. Chem. Technol. Biotechnol.* **1999**, *74*, 852.
(101) Cammi, R.; Mennucci, B.; Tomasi, J. *J. Phys. Chem. A* **2000**, *104*, 5631.
(102) Mennucci, B.; Cammi, R.; Tomasi, J. *J. Chem. Phys.* **1998**, *109*, 2798.
(103) Cossi, M.; Barone, V. *J. Chem. Phys.* **2000**, *112*, 2427.
(104) Aguilar, M. A. *J. Phys. Chem. A* **2001**, *105*, 10393.
(105) PF can also accept an H-bond in H-bonding solvents. According to our quantum chemical calculations, such a bond may slightly reduce the Stokes shift and the reorganization energy (Supporting Information, Section 1.7S). Such a bond should be sterically less favorable in *N*-methyl formamide, explaining its proximity to the non-H-bonding solvents in Figure 2.
(106) The anomalously high solvent reorganization energy disappears in mixtures of water with cosolvents. Upon addition of a small amount of nonanomalous solvents (e.g., DMSO, acetonitrile, methanol) to water, we observed a decrease in λ_s of an order of magnitude larger than expected from the change in the macroscopic ϵ_{st} and ϵ_{op} of these mixtures. Such an effect was not observed in mixtures of nonanomalous solvents (e.g., λ_s is practically independent of mixture composition in methanol−acetonitrile mixtures). An anomalously high dielectric response of water was also observed for PF bound inside a water-soluble, globular protein where the dye was not in direct contact with water.[116] Similar to free PF in water, cosolvents rapidly destroy the anomaly for the bound dye. This effect does not seem to be related to cosolvent adsorption (no cosolvent adsorption to the surface of this protein was observed, Topolev, V. V.; Krishtalik, L. I. *Biofizika* **1999**, *44*, 992−995) or to a change in the protein conformation, Khurgin, I. I.; Azizov, I. M.; Abaturov, L. V.; Kogan, G. A.; Rosliakov, V. I. *Biofizika* **1972**, *17*, 390−395. A detailed account of the cosolvent effect will be published elsewhere.
(107) Ladanyi, B. M.; Skaf, M. S. *Annu. Rev. Phys. Chem.* **1993**, *44*, 335.
(108) We estimated the ratio of the dipolar components of λ_s for C153 and PF to be $(\Delta\mu_{C153} = 4.5D/\Delta\mu_{PF} = 1.3D)^2 \approx 12$, on the basis of the gas-phase TD/MPW1PW1/6-31G(d,p) calculation and the similarity of the sizes of these probes.
(109) Ma, J.; Bout, D. V.; Berg, M. *J. Chem. Phys.* **1995**, *103*, 9146.
(110) Until recent publications of the rigorous DCM approach,[24,25] DCM-based analyses involved either uniform dielectric (Pekar parameter), point-dipole/spherical-cavity (Lippert−Mataga parameter), or "fixed displacement field" approximations (see ref 24 for discussion). Previous DCM calculations also used other approximations such as neglecting solute electronic polarizability and atomic point charge representation of charge redistribution. We will show in a separate publication that the experimental functional relationship $\lambda_s(\epsilon_{op},\epsilon_{st})$ and overall magnitude of λ_s can be reproduced without the extensive quantum chemical calculations presented here, if the number of partial charges, significantly larger than the number of atoms, accounting for polarizability of the detailed molecular cavity is used within the rigorous DCM approach. Neglecting these factors can cause apparent deviations from DCM, which can be mild (as for the uniform, smeared-charge approximation, Table 1) or strong, as for PF′ λ_s underestimated by an order of magnitude within the molecular cavity model with standard atomic charges fitting the electrostatic potential. To reproduce $\lambda_s(\epsilon_{op},\epsilon_{st})$ only, 2−4 charges corresponding to the largest atomic charges in a polarizable oblate spheroid cavity can be used for C153 and PF instead.
(111) Newton, M. D.; Basilevsky, M. V.; Rostov, I. V. *Chem. Phys.* **1998**, *232*, 201.
(112) Matyushov, D. V. *Chem. Phys.* **1993**, *174*, 199.
(113) For example, within the point dipole in the spherical cavity approximation usually used to analyze solvatochromism within the macroscopic model, the solvent reorganization energy is proportional to the Lippert−Mataga parameter, $\lambda_s(\epsilon_{op},\epsilon_{st}) \propto (\epsilon_{st}/\epsilon_c-1)/(2\epsilon_{st}/\epsilon_c + 1) - (\epsilon_{op}/\epsilon_c-1)/(2\epsilon_{op}/\epsilon_c + 1)$. The sign of the temperature derivative of this parameter changes depending on whether the solute polarizability is neglected (cavity dielectric constant $\epsilon_c = 1$) or not ($\epsilon_c \approx 2.5$). This is the case for acetonitrile analyzed in ref 9.
(114) It follows from the response theory that equilibrium density changes in response to static electric field are identically zero for the linear response of a solvent whose electrically neutral molecules have antisymmetric charge density and symmetric nonelectrostatic potential with respect to the molecule center (e.g., a dipole inside a sphere), because the density change in such a solvent may not depend on inversion of the electric field direction. For asymmetric solvent molecules, linear density changes are not forbidden.

(115) See a compilation of solvent acidity scales: Catalan, J.; Gomez, J.; Saiz, J. L.; Couto, A.; Ferraris, M.; Laynez, J. *J. Chem. Soc., Faraday Trans. 2* **1995**, *12*, 2301.

(116) Mertz, E. L.; Krishtalik, L. I. *Proc. Natl. Acad. Sci.* **2000**, *97*, 2081.

(117) Our data suggest that the anomaly is also present in acridine orange (AO), a dye that is similar to PF, except the two NH_2 groups are replaced by two $N(CH_3)_2$ groups. Although the first solvation shell of AO is somewhat different because of different dye−solvent H-bonding, λ_s for AO is also markedly higher in water than in other solvents (e.g., methanol and acetonitrile). The anomalously high λ_s for AO in water is also accompanied by an anomalous solvent isotope effect. This effect is not observed in methanol.

(118) Bagchi, B.; Chandra, A. *Adv. Chem. Phys.* **1991**, *80*, 1.

(119) The qualitative failure of the smeared-charge model is a result of the strong sensitivity of the calculated response energies to the position and height of peaks in the response function $\chi(k)$, which are quite different for different solvents, Figure 6. Even stronger sensitivity was reported for the dielectric approximation where calculated energy can diverge upon a slight change in $\chi(k)$.[30] We also found similar sensitivity for the specular reflection model. Thus, all these heuristic models are in qualitative disagreement with the data.

(120) A modification of heuristic dielectric approximation can produce sensible solvation energies of small ions in water, if an additional fitting function that strongly depends on the solvent $\chi(k)$ is introduced.[30] It is unclear whether such energies containing significant nondielectric contributions from ion−solvent electron donor−acceptor interactions and from the solvent pre-existing potential can be described in terms of the solvent dielectric properties. Furthermore, the fitting function directly couples changes in solute cavity size to solute charge. We are not aware of any indication that such direct interaction between solute electric field and mass (solvent density near solute) is important. In contrast, such coupling, if it exists, seems to be insignificant for our probe, because the measured reorganization energies are almost insensitive to pressure; Sections 4.1 and 5.

(121) The still-popular Lorentzian approximation of $\chi(k)$ at small values of k does not provide a consistent description of the data (Section 4.2). Furthermore, this approximation underestimates $\chi(k)$ by two orders of magnitude at k's where the probes' charge redistributions $\Delta\rho(k)$'s have significant components (Figure 6). Finally, it is unclear if the condition for the approximation $c = d\chi(k)/dk|_{k\to 0} < 0$ holds for dipolar solvents, because the sign of c obtained from molecular simulations strongly depends on an approximation of solvent intramolecular charge density,[86] Kornyshev, A. A.; Sutmann, G. *J. Mol. Liq.* **1999**, *82*, 151.

(122) Soper, A. K.; Finney, J. L. *Phys. Rev. Lett.* **1993**, *71*, 4346.

(123) Keller, W.; Morgner, H.; Muller, W. A. *Mol. Phys.* **1986**, *57*, 623.

(124) Wojcik, M. C.; Hermansson, K.; Siegbahn, H. O. G. *J. Chem. Phys.* **2000**, *113*, 3374.

(125) Wilson, K. R.; Schaller, R. D.; Co, D. T.; Saykally, R. J.; Rude, B. S.; Catalano, T.; Bozek, J. D. *J. Chem. Phys.* **2002**, *117*, 7738.

(126) Scatena, L. F.; Brown, M. G.; Richmond, G. L. *Science* **2001**, *292*, 908.

(127) Du, Q.; Freysz, E.; Shen, Y. R. *Science* **1994**, *264*, 826.

(128) Lee, S. H.; Rossky, P. J. *J. Chem. Phys.* **1994**, *100*, 3334.

(129) Oberbrodhage, J.; Morgner, H.; Tapia, O.; Siegbahn, H. O. G. *Int. J. Quantum Chem.* **1997**, *63*, 1123.

(130) Because length scales of charge redistribution are different for different probes, the anomaly may be seen with some probes and not seen with others. For example, the anomaly is observed for PF in formamide, but no anomaly is observed for another probe C153 in formamide.[11] Like other traditional dipolar or ionic probes, the dominating component of the C153′ charge redistribution has the range of length scales (2.5−25 Å) which are longer than those of PF (1−2.5 Å).[108] The absence of an anomalous response for C153 may be explained (e.g., assuming that anomalous polarization fluctuations occur at 1−2.5 Å length scales, which is within the range of charge redistribution of PF and outside the range of C153).

(131) Experimental values of total response energies W's were recovered from the solvent dependence of the redox potential difference $\Delta\psi = \text{const} + 2W$ as $W = (1 - \epsilon_{st}^{-1})d\Delta\psi/d\epsilon_{st}^{-1}/2$, because W was shown to obey DCM (i.e., Born equation $W = (1 - \epsilon_{st}^{-1})e^2/2a_{vdw}$ with van der Waals radius $a_{vdw} = 3.7$ Å)[1].

(132) For the sake of illustration, we generated W and λ_s values measured in several solvents plotted in Figure 5, because $\chi(k)$'s of few experimentally studied solvents are available. The generated W and λ_s values were obtained from the established correlation between the data and the DCM model (Figures 2, 4; Sections 4.1, 4.2) and macroscopic λ_s^{cal} and W^{cal} values calculated in tetrahydrofuran, chloroform, and methyl acetate (for PF and Cp_2Co), benzonitrile (PF, C153, Cp_2Co), methanol (Cp_2Co), and water (C153, Cp_2Co). We verified that the inclusion of these generated data into the analysis presented in Table 1 would produce similar results.